Numerical analysis of fluid flow problems using spectral relaxation method (SRM)

GILBERT MAKANDA
Central University of Technology, Free State,
Private Bag X20539, Bloemfontein, 9300
SOUTH AFRICA

Abstract: The paper presents four examples arising from mathematical models in fluid flow. Examples 1 and 2 illustrate the implementation of the spectral relaxation method (SRM) on problems involving ordinary differential equations. Examples 3 and 4 illustrate the application of the SRM on partial differential equations. The SRM is accurate and robust if it is used together with the successive over-relaxation (SOR) technique. The method is easy to implement and requires less computational time than similar methods that can be used to solve similar problems. The method converges after a few iterations and is stable. The method can be used as an alternative method to solve problems arising in fluid flow.

Keywords: Successive relaxation, spectral relaxation method, ordinary and partial differential equations

Received: July 18, 2021. Revised: August 5, 2022. Accepted: September 5, 2022. Published: October 11, 2022.

1. Introduction

Spectral methods were mostly developed in the 1970s. They have played an important role in recent studies of numerical solutions of differential equations in regular domains. They are considered to be efficient due to their high accuracy [1]. According to Vilhena et al. [2], spectral methods encompass representing the solution to the problem as truncated series of known functions of independent variables. Spectral methods that make use of collocation methods are usually called pseudo-spectral methods [3], and these methods have been widely used [4]. The collocation points are normally the zeros of the polynomial chosen for approximation [5]. In the case of Chebyshev collocation method, the collocation points chosen are the Gauss-Lobatto points [6], [7], [8], [9]. The Chebyshev Gauss-Lobatto nodes have also been used in Rashad [10]. More recently, Legendre and Chebyshev spectral approximations have been used in PDEs in bounded domains [1].

Some progress have been made in solving problems in unbounded domains. In particular, Tatari and Haghighi [1] investigated Laguerre and Hermite polynomials and used appropriate choices for semi-infinite and infinite domains. Specifically, an accurate Christov-Galerkin spectral technique for the solutions of interacting localized wave solutions of fourth and sixth order generalized wave equations was achieved by application of spectral methods on an infinite domain [11]. The use of spectral methods has been motivated by their accuracy and robustness in solving incompressible Navier-Stokes equations [12]. Some approximations like the Galerkin approximations or collocation schemes have been described by [13]. The main advantage of the method is that there is no need for numerical integration [14]. Thus, spectral methods provide more accurate solution approximations with a small number of unknowns, and so play important roles in optimizing engineering designs and other scientific computations [15].

Spectral methods are applied in numerical solutions for neutron transport [16], Darcy and coupled Stokes equations [17], modelling of bridges [18]. Pozrikidis [19] applied spectral collocation method with triangular boundary elements for solving integral equations arising from boundary integral formulations over surfaces discretized into flat or curved triangular elements. Dlamini et al. [20] compared the pseudo-spectral method and the compact finite difference (CFD) method for solving boundary layer problems and found that the spectral method were better than the CFD in terms of computational speed.

Other applications of spectral methods are in the spectral local linearization method (SLLM), spectral relaxation method (SRM), the spectral quasi-linearization method (SQLM), the spectral perturbation method (SPM), the bivariate quasi-linearization method (BQLM/BSQLM). Most of these methods are based on linearization methods. The spectral relaxation method (SRM) requires converting the equations into a system of first order differential equations [21] or arranging the equations in a particular order, placing the equations with least number of unknowns at the top of the equation list [22]. The resulting system is then decoupled using ideas from the Gauss-Seidel method, which is normally used to solve linear algebraic systems of equations [9]. The decoupled system is numerically integrated using the Chebyshev pseudo spectral method [6]. Unlike other iterative schemes for solving nonlinear differential equations, the SRM does not require any evaluation of derivatives and perturbation [9]. Developments of the SRM are noted in [20] where a multistage spectral relaxation method is used for solving problems of chaos control and synchronization. Thus, the SRM is an efficient, reliable, convergent, numerically stable and very easy method to implement that has a great potential as very useful tool for solving boundary layer flow problems arising from fluid dynamics applications [9]. In this study we implement the spectral relaxation method (SRM). From the literature mentioned above, it is clear that this method is highly accurate as well as easy to implement.

1.1 Spectral relaxation method (SRM)

In this section we give a detailed description of the spectral relaxation method as described in Motsa et al. [32]. We consider a system of n nonlinear ordinary differential equations in n unknown functions $f_i(\eta)$, $i = 1, 2, \ldots n$ where $\eta \in [a, b]$ is the dependent variable. We define a vector $\boldsymbol{F}_i$ to be a vector of derivatives of the variable f_i with respect to η

$$\boldsymbol{F}_i(\eta) = \left[f_i^{(0)}, f_i^{(1)}, \ldots, f_i^{(m_i)}\right]. \tag{1}$$

Where $f_i^{(0)} = f_i$, $f_i^{(p)}$, is the pth derivative of f_i with respect to η and $m_i (i = 1, 2, 3 \ldots, n)$ is the highest derivative order of the variable f_i which is in the system of equations. The system can be written in terms of $\boldsymbol{F}_i$ as the sum of linear ($\mathcal{L}_i$) and nonlinear components ($\mathcal{N}_i$) as

$$\begin{aligned}\mathcal{L}_i\left[F_1, F_2, \ldots, F_n\right] + \mathcal{N}_i\left[F_1, F_2, \ldots, F_n\right] \\ = \mathcal{G}_i(\eta),\ i = 1, \ldots n.\end{aligned} \tag{2}$$

Where $\mathcal{G}(\eta)$ is a known function of η.

Eq. (2) is solved subject to two point boundary conditions which are expressed as

$$\sum_{j=1}^{n}\sum_{p=0}^{m_j-1}\alpha_{\nu,j}^{(p)} f_j^{(p)}(a) = K_{a,\nu},\ \nu = 1, 2, \ldots, n_a, \tag{3}$$

$$\sum_{j=1}^{n}\sum_{p=0}^{m_j-1}\gamma_{\nu,j}^{(p)} f_j^{(p)}(b) = K_{b,\sigma},\ \sigma = 1, 2, \ldots, n_b, \tag{4}$$

where $\alpha_{\nu,j}^{(p)}$, $\gamma_{\sigma,j}^{(p)}$ are the constant coefficients of $f_j^{(p)}$ in the boundary conditions, and n_a and n_b are the total number of prescribed boundary conditions at $\eta = a$ and $\eta = b$ respectively. Starting from the initial approximation $\boldsymbol{F}_{1,0}, \boldsymbol{F}_{2,0}, \ldots, \boldsymbol{F}_{n,0}$, the iterative method is obtained as

$$\begin{aligned}
&\mathcal{L}_1\left[F_{1,r+1}, F_{2,r}, \ldots, F_{n,r}\right] = G_1 \\
&\quad + \mathcal{N}_1\left[F_{1,r}, F_{2,r}, \ldots, F_{n,r}\right], \\
&\mathcal{L}_2\left[F_{1,r+1}, F_{2,r+1}, \ldots, F_{n,r}\right] = G_2 \\
&\quad + \mathcal{N}_2\left[F_{1,r+1}, F_{2,r}, \ldots, F_{n,r}\right], \\
&\vdots\ \vdots \quad \vdots \quad \vdots \quad \vdots \quad \vdots\ \vdots \quad \vdots \quad \vdots \quad \vdots \\
&\mathcal{L}_{n-1}\left[F_{1,r+1}, F_{2,r+1}, \ldots, F_{n-1,r+1}, F_{n,r}\right] = G_{n-1} \\
&\quad + \mathcal{N}_{n-1}\left[F_{1,r+1}, \ldots, F_{n-2,r+1}, F_{n-1,r}, F_{n,r}\right], \\
&\mathcal{L}_n\left[F_{1,r+1}, F_{2,r+1}, \ldots, F_{n-1,r+1}, F_{n,r+1}\right] = G_n \\
&\quad + \mathcal{N}_n\left[F_{1,r}, F_{2,r}, \ldots, F_{n,r}\right].
\end{aligned} \tag{5}$$

Where $\boldsymbol{F}_{i,r+1}$ and $\boldsymbol{F}_{i,r}$ are the approximation of $\boldsymbol{F}_i$ at the current and the previous iterations respectively. We state that Eqs. (5) form a system of n linear decoupled equations which can be solved iteratively for $r = 1, 2 \ldots$. We start from a an appropriate initial approximation $F_{i,0}$ which satisfy boundary conditions. The iterations are repeated until convergence is reached. The decoupling error can be used to assess the desired convergence. The decoupling error E_r at the $(r+1)$th iteration is defined by

The idea incorporated in this method is the Gauss-Seidel relaxation method which is normally used for solving large systems of algebraic equations. To implement the spectral collocation method, we define the differentiation matrix

$$\frac{df_i(\eta_l)}{d\eta} = \sum_{k=0}^{N}\mathbf{D}_{l,k} f_i(\tau_k) = \mathbf{D}\ \mathbf{F}_i, l = 0, \ldots, N. \tag{6}$$

Where $N + 1$ is the number collocation points, $\mathbf{D} = 2D/(b - a)$ and
$\mathbf{F} = \left[f(\tau_0), f(\tau_1), \ldots, f(\tau_N)\right]^T$ is the vector function of the collocation points and higher order derivatives are obtained in powers of $\mathbf{D}$ given by

$$f_j^{(p)} = \mathbf{D}^p\mathbf{F}_j. \tag{7}$$

We then apply the Chebyshevpseudo spectral method to the iteration scheme shown in Eqs. (5)-(5). This then gives

$$\sum_{j=1}^{n}\sum_{p=0}^{m_j}\beta_{i,j}^{[p]} f_j^{(p)} + \mathcal{N}_i\left[\boldsymbol{F}_1, \boldsymbol{F}_2, \ldots, \boldsymbol{F}_n\right] = G_i, \tag{8}$$

where $\beta_{i,j}^{(p)}$ are constants coefficients of $f_j^{(p)}$, the derivative of $f_j (j = 1, 2, \ldots, n)$ that is in the ith equation for $i = 1, 2, \ldots, n$. The iteration scheme used in Eqs.(5-5) can be expressed as

$$\begin{aligned}\sum_{j=1}^{i}\sum_{p=0}^{n_j}\beta_{i,j}^{[p]} f_{j,r+1}^{(p)} = \mathcal{G}_i - \sum_{j=1+1}^{m}\sum_{p=0}^{n_j}\beta_{i,j}^{[p]} f_{j,r+1}^{(p)} \\ -\mathcal{N}_i\left[F_{1,r+1}, \ldots, F_{i-1,r+1}, F_{i,r}, \ldots, F_{m,r}\right]\end{aligned} \tag{9}$$

for $i = 1, 2, \ldots, m$. Using the Eq. (8) on Eq. (9) and the boundary conditions we otain the spectral Gauss-Seidel relaxation method iteration scheme given by

$$\sum_{j=1}^{i}\sum_{p=0}^{m_j}\beta_{i,j}^{[p]}\mathbf{D}^{(p)}\mathbf{F}_{j,r+1} = \mathcal{G}_{\mathbf{i}} - \sum_{\mathbf{j=1+1}}^{\mathbf{n}}\sum_{\mathbf{p=0}}^{\mathbf{m_j}}\beta_{\mathbf{i,j}}^{[\mathbf{p}]}\mathbf{D^{(p)}F_{j,r}} - \mathcal{N}_i\left[\mathbf{F}_{1,r+1},\ldots,\mathbf{F}_{i-1,r+1},\mathbf{F}_{i,r},\ldots,\mathbf{F}_{n,r}\right], \quad (10)$$

subject to

$$\sum_{j=1}^{i}\sum_{p=0}^{m_j-1}\alpha_{\nu,j}^{(p)}\sum_{k=0}^{N}\mathbf{D}_{N,k}^{p}f_{j,r+1}(\tau_k) = K_{a,\nu}, \quad \nu = 1,2,\ldots,n_a, \quad (11)$$

$$\sum_{j=1}^{n}\sum_{p=0}^{m_j-1}\gamma_{\sigma,j}^{[p]}\sum_{k=0}^{N}\mathbf{D}_{N,k}^{p}f_{j,r+1}(\tau_k) = K_{b,\sigma}, \quad \sigma = 1,2,\ldots,n_b, \quad (12)$$

The substitution of previously known functions decouples the system of equations and an efficient iteration scheme is created giving accurate results. The spectral relaxation method (SRM) will be implemented in the next section.

Numerical examples

2. Example 1: Boundary layer free convection flow from a spinning cone under magnetic field

In this section we demonstrate the implementation of the spectral relaxation method, we give two examples of applications in ordinary differential equations and two examples of applications in partial differential equations. We begin by considering the problem of Ece [24]; free convection flow about a vertical spinning cone under a magnetic field. The problem is fully described in Ece [24]. The governing equations are written as

$$\frac{\partial(ru)}{\partial x} + \frac{\partial(rv)}{\partial y} = 0 \quad (13)$$

$$u\frac{\partial u}{\partial x} + v\frac{\partial u}{\partial y} - \frac{Re^2}{Gr}\frac{r'w^2}{r} = \frac{\partial^2 u}{\partial y^2} + \Theta - M\Lambda^2 u, \quad (14)$$

$$u\frac{\partial w}{\partial x} + v\frac{\partial w}{\partial y} - uw\frac{r'}{r} = \frac{\partial^2 w}{\partial y^2} - M\Lambda^2 u, \quad (15)$$

$$u\frac{\partial \Theta}{\partial x} + v\frac{\partial \Theta}{\partial y} = \frac{1}{Pr}\frac{\partial^2\Theta}{\partial y^2}, \quad (16)$$

where the rotational Reynolds number Re, the magnetic field function Λ and the magnetic parameter M are given by

$$Re = \frac{\Omega L^2}{\nu},\ \Lambda = \frac{b(x)}{r\sqrt{1-r^2}},\ M = \frac{\sigma B_0^2 L}{U\rho}, \quad (17)$$

where σ is the electrical conductivity and ρ is the density of the fluid. Boundary conditions considered are as follows;

$$u(x,0) = 0,\ v(x,0) = 0,\ w(x,0) = r,\ \Theta(x,0) = a(x), \quad (18)$$

$$u(x,y) \to 0,\ w(x,y) \to 0,\ \Theta(x,y) \to 0 \text{ as } y \to \infty, \quad (19)$$

where

$$a(x) = [A(x) - T_0]/(T_r - T_0), \quad (20)$$

$$c(x) = Gr^{-\frac{1}{4}}C(x)/k(T_r - T_0) \quad (21)$$

Using the stream function and boundary layer variables defined as

$$ru = \frac{\partial\psi}{\partial y},\ rv = -\frac{\partial\psi}{\partial x}, \quad (22)$$

$$\psi(x,y) = xrF(y),\ w = rG(y),\ \Theta = xH(y). \quad (23)$$

where $r = x\sin\phi$.

we obtain the following ordinary differential equations as in Ece[24],

$$F''' + 2FF'' - F'^2 - MF' + \epsilon G^2 + H = 0, \quad (24)$$

$$G'' + 2FG' - 2F'G - MG = 0, \quad (25)$$

$$\frac{1}{Pr}H'' + 2FH' - F'H = 0, \quad (26)$$

where $\epsilon = (Re\sin\phi)^2/Gr$ is the spin parameter, the boundary conditions considered in this example are given as;

$$F(0) = 0,\ F'(0) = 0, G(0) = 1, H(0) = 1, \quad (27)$$

$$F'(y) \to 0,\ G(y) \to 0,\ H(y) \to 0 \text{ as } y \to \infty. \quad (28)$$

Applying the SRM as described in section A. in equations (24) - (26) and first reducing it to a system of second order equations we obtain,

$$F' = K, \quad (29)$$

$$K'' + 2fK' - K^2 - MK + \epsilon G^2 + H = 0, \quad (30)$$

$$G'' + 2FG' - 2F'G - MG = 0, \quad (31)$$

$$\frac{1}{Pr}H'' + 2FH' - F'H = 0, \quad (32)$$

with boundary conditions

$$F(0) = 0,\ K(0) = 0, G(0) = 1, H(0) = 1, \quad (33)$$

$$K(y) \to 0,\ G(y) \to 0,\ H(y) \to 0 \text{ as } y \to \infty. \quad (34)$$

The iterative scheme for the system (29) -(32) becomes

$$F'_{r+1} = K_r, F_{r+1}(0) = 0 \quad (35)$$

$$K''_{r+1} + 2f_{r+1}K'_{r+1} - MK_{r+1} = K_r^2 - \epsilon G_r^2 - H_r, \quad (36)$$

$$G''_{r+1} + 2F_{r+1}G'_{r+1} - 2K_{r+1}G_{r+1} - MG_{r+1} = 0, \quad (37)$$

$$\frac{1}{Pr}H''_{r+1} + 2F_{r+1}H'_{r+1} - K_{r+1}H_{r+1} = 0, \quad (38)$$

with boundary conditions

$$F_{r+1}(0) = 0,\ K_{r+1}(0) = 0, G_{r+1}(0) = 1, \quad H_{r+1}(0) = 1, \tag{39}$$

$$K_{r+1}(y) \to 0,\ G_{r+1}(y) \to 0, \quad H_{r+1}(y) \to 0 \text{ as } y \to \infty. \tag{40}$$

Applying the Chebyshev pseudospectral method on system (35) -(38) we obtain

$$A_1\mathbf{F}_{r+1} = B_1, F_{r+1}(\tau_N) = 0, \tag{41}$$

$$A_2\mathbf{K}_{r+1} = B_2, K_{r+1}(\tau_N) = 0, K_{r+1}(\tau_0) = 0, \tag{42}$$

$$A_3\mathbf{G}_{r+1} = B_3, G_{r+1}(\tau_N) = 1, G_{r+1}(\tau_0) = 0, \tag{43}$$

$$A_4\mathbf{H}_{r+1} = B_4, H_{r+1}(\tau_N) = 0, H_{r+1}(\tau_0) = 0, \tag{44}$$

where

$$\mathbf{A}_1 = \mathbf{D}, \mathbf{B}_1 = K_r, \tag{45}$$

$$\mathbf{A}_2 = \mathbf{D}^2 + 2\text{diag}F_{r+1}\mathbf{D} - MI, \tag{46}$$

$$\mathbf{B}_2 = K_r^2 - \epsilon G_r^2 - H_r, \tag{47}$$

$$\mathbf{A}_3 = \mathbf{D}^2 + 2\text{diag}F_{r+1}\mathbf{D} - 2\text{diag}K_{r+1}, \tag{48}$$

$$\mathbf{B}_3 = 0, \tag{49}$$

$$\mathbf{A}_4 = \frac{1}{Pr}\mathbf{D}^2 + 2\text{diag}F_{r+1}\mathbf{D} - \text{diag}K_{r+1}, \tag{50}$$

$$\mathbf{B}_4 = 0, \tag{51}$$

3. Improving the convergence of the spectral relaxation method

We use the successive over-relaxation (SOR) method to accelerated the convergence rates of the spectral relaxation method. This method is normally used in numerical linear algebra to control the convergence of the Gauss-Seidel method for linear systems of equations. In this section we propose a similar method to improve the convergence of the spectral relaxation method. If the SRM scheme for solving a function x at the $(r+1)$th iteration is

$$\mathbf{a}x_{r+1} = \mathbf{b}, \tag{52}$$

We define the modified version of the SRM as

$$\mathbf{a}x_{r+1} = (1-\omega)\mathbf{a}x_r + \omega\mathbf{b}, \tag{53}$$

where $\mathbf{a}, \mathbf{b}$ are matrices and ω is the convergence controlling relaxation parameter. The case $\omega = 1$ reduce the system (53) to (52). when $\omega < 1$ convergence speeds up and slows down when $\omega > 1$. The effect of changing ω will be discussed in the results and discussion section.

4. Example 2: Free convection from an inverted cone in porous medium with cross diffusion effects

We considering the problem of Awad et al. [25] which investigated free convection flow from an inverted cone in porous medium with cross diffusion, the governing equations were presented as;

$$\frac{\partial(ru)}{\partial x} + \frac{\partial(rv)}{\partial y} = 0 \tag{54}$$

$$u\frac{\partial u}{\partial x} + v\frac{\partial u}{\partial y} = \nu\frac{\partial^2 u}{\partial y^2} - \frac{\nu}{K}u - g\beta\cos\Omega(T - T_\infty) + g\beta^*\cos\Omega(C - C_\infty) \tag{55}$$

$$u\frac{\partial T}{\partial x} + v\frac{\partial T}{\partial y} = \alpha\frac{\partial^2 T}{\partial y^2} + \frac{Dk}{C_sC_p}\frac{\partial^2 C}{\partial y^2}, \tag{56}$$

$$u\frac{\partial C}{\partial x} + v\frac{\partial C}{\partial y} = D\frac{\partial^2 C}{\partial y^2} + \frac{Dk}{C_sC_p}\frac{\partial^2 T}{\partial y^2}, \tag{57}$$

where $r = x\sin\Omega$, u and v are velocity components in the x and y directions respectively. ρ is the fluid density, g is the acceleration due to gravity, K is the permeability, ν is the kinematic viscosity of the fluid. β and β^* are the thermal expansion and concentration expansion coefficients respectively. α and D are thermal and mass diffusivities, k is the thermal diffusion ratio. c_p is the specific heat capacity at constant pressure and c_s is the concentration susceptibility. The boundary conditions are given by

$$\begin{aligned} &u = 0,\ v = 0, T = T_w = T_\infty + Ax^\lambda, \\ &C = C_w = C_\infty + Bx^\lambda,\ \text{on } y = 0,\ x > 0, \\ &u = 0,\ T = T_\infty,\ C = C_\infty,\ \text{as } y \to \infty \end{aligned} \tag{58}$$

where $A, B > 0$ are constants and λ is the power-law index. By using the similarity transformations and stream functions described in Awad et.al [25], we obtain the following system of ordinary differential equations.

$$f''' + \left(\frac{\lambda+7}{4}\right)ff'' - \left(\frac{\lambda+1}{2}\right)f'^2 - \Lambda f' + \theta + N_1\phi = 0, \tag{59}$$

$$\theta'' + D_f\phi'' + Pr\left(\frac{\lambda+7}{4}\right)f\theta' - Pr\lambda f'\theta = 0, \tag{60}$$

$$\phi'' + S_r\theta'' + Sc\left(\frac{\lambda+7}{4}\right)f\phi' - Sc\lambda f'\phi = 0, \tag{61}$$

with boundary conditions given as

$$\begin{aligned} &f = 0,\ f' = 0, \theta = \phi = 1,\ \text{on } \eta = 0, \\ &f' = 0,\ \theta = 0,\ \phi = 0,\ \text{as } \eta \to \infty \end{aligned} \tag{62}$$

where D_f is the Dufour number, Sr is the Soret number, N_1 is the buoyancy parameter, Pr is the Prandtl number, Sc is the Schmidt number. To solve the system (59) - (62), we first substitute for θ'' in equation (61) and for ϕ'' in equation (60) reduces to the following system,

$$f''' + \left(\frac{\lambda+7}{4}\right) ff'' - \left(\frac{\lambda+1}{2}\right) f'^2 - \Lambda f' + \theta + N_1\phi = 0, \quad (63)$$

$$(1 - D_f S_r)\theta'' - ScD_f\left(\frac{\lambda+7}{4}\right) f\phi' + ScD_f\lambda f'\phi + Pr\left(\frac{\lambda+7}{4}\right) f\theta' - Pr\lambda f'\theta = 0, \quad (64)$$

$$(1 - D_f S_r)\phi'' - SrPr\left(\frac{\lambda+7}{4}\right) f\theta' + SrPr\lambda f'\theta + Sc\left(\frac{\lambda+7}{4}\right) f\phi' - Sc\lambda f'\phi = 0, \quad (65)$$

subject to boundary conditions

$$f = 0,\ f' = 0, \theta = \phi = 1,\ \text{on } \eta = 0,$$
$$f' = 0,\ \theta = 0,\ \phi = 0,\ \text{as } \eta \to \infty \quad (66)$$

We now apply the spectral relaxation technique as follows, the system is converted yo a system of second order ordinary differential equations. The iterative system as written as;

$$f'_{r+1} = g_r, f_{r+1}(0) = 0, \quad (67)$$

$$g''_{r+1} + \left(\frac{\lambda+7}{4}\right) f_{r+1}g'_{r+1} - \Lambda g_{r+1} = \left(\frac{\lambda+1}{2}\right) g_r^2 - \theta_r - N_1\phi_r, \quad (68)$$

$$(1 - D_f S_r)\theta''_{r+1} - Pr\left(\frac{\lambda+7}{4}\right) f_{r+1}\theta' - Pr\lambda g_{r+1}\theta_{r+1} = ScD_f\left(\left(\frac{\lambda+7}{4}\right) f_{r+1}\phi'_r - \lambda g_{r+1}\phi_r\right), \quad (69)$$

as

$$(1 - D_f S_r)\phi''_{r+1} - Sc\left(\frac{\lambda+7}{4}\right) f_{r+1}\phi' - Sc\lambda g_{r+1}\phi_{r+1} = SrPr\left(\left(\frac{\lambda+7}{4}\right) f_{r+1}\theta'_{r+1} - \lambda g_{r+1}\theta_{r+1}\right) \quad (70)$$

subject to

$$g_{r+1}(0) = 0,\ g_{r+1}(\infty) = 0, \theta_{r+1}(0) = 1,$$
$$\phi_{r+1}(0) = 1,\ \phi_{r+1}(\infty) = 0. \quad (71)$$

Applying the Chebyshev pseudospectral method on system (67) -(71) we obtain

$$A_1\mathbf{f}_{r+1} = B_1, f_{r+1}(\tau_N) = 0, \quad (72)$$
$$A_2\mathbf{g}_{r+1} = B_2, g_{r+1}(\tau_N) = 0, g_{r+1}(\tau_0) = 0, \quad (73)$$
$$A_3\theta_{r+1} = B_3, \theta_{r+1}(\tau_N) = 1, \theta_{r+1}(\tau_0) = 0, \quad (74)$$
$$A_4\phi_{r+1} = B_4, \phi_{r+1}(\tau_N) = 0, \phi_{r+1}(\tau_0) = 0, \quad (75)$$

where

$$\mathbf{A}_1 = \mathbf{D}, \mathbf{B}_1 = g_r, f_{r+1}(\tau_{\bar{N}}) = 0, \quad (76)$$
$$\mathbf{A}_2 = \mathbf{D}^2 + \left(\frac{\lambda+7}{4}\right)\text{diag}f_{r+1}\mathbf{D} - \Lambda\mathbf{I}, \quad (77)$$
$$\mathbf{B}_2 = g_r^2 - \theta_r^2 - N_1\phi_r, \quad (78)$$
$$g_{r+1}(\tau_{\bar{N}}) = 0,\ g_{r+1}(\tau_0) = 0. \quad (79)$$
$$\mathbf{A}_3 = (1 - D_f S_r)\mathbf{D}^2 + Pr\left(\frac{\lambda+7}{4}\right)\text{diag}f_{r+1}\mathbf{D} - Pr\lambda\text{diag}g_{r+1}, \quad (80)$$
$$\mathbf{B}_3 = ScD_f\left(\left(\frac{\lambda+7}{4}\right) f_{r+1}\phi'_r - \lambda g_{r+1}\phi_r\right), \quad (81)$$
$$\theta_{r+1}(\tau_{\bar{N}}) = 0,\ \theta_{r+1}(\tau_0) = 0. \quad (82)$$
$$\mathbf{A}_4 = (1 - D_f S_r)\mathbf{D}^2 + Sc\left(\frac{\lambda+7}{4}\right)\text{diag}f_{r+1}\mathbf{D} - Sc\lambda\text{diag}g_{r+1}, \quad (83)$$
$$\mathbf{B}_4 = SrPr\left(\left(\frac{\lambda+7}{4}\right) f_{r+1}\theta'_{r+1} - \lambda g_{r+1}\theta_{r+1}\right) \quad (84)$$
$$\phi_{r+1}(\tau_{\bar{N}}) = 0,\ \phi_{r+1}(\tau_0) = 0. \quad (85)$$

5. Example 3: Non-Darcy unsteady mixed convection flow near the stagnation point on a heated vertical surface embedded in porous medium with thermal radiation and variable viscosity

A semi-infinite vertical plate placed in a saturated porous medium with uniform ambient temperature T_∞, at time $t = 0$ the fluid is impulsively moved with velocity U_e and the surface temperature is suddenly raised.

The governing equations in this fluid flow are given

$$\frac{\partial u}{\partial x} + \frac{\partial v}{\partial y} = 0, \quad (86)$$

$$\frac{\partial u}{\partial t} + u\frac{\partial u}{\partial x} + v\frac{\partial u}{\partial y} = U_e\frac{\partial U_e}{\partial x} + \frac{1}{\rho}\frac{\partial}{\partial y}\left(\mu\frac{\partial u}{\partial y}\right) + g\beta_T(T - T_\infty) + \frac{\epsilon}{\rho K}(\mu_\infty U_\infty - \mu u) + \frac{F_1\epsilon^2}{K^{\frac{1}{2}}}(U_e^2 - u^2) \quad (87)$$

$$\frac{\partial T}{\partial t} + u\frac{\partial T}{\partial x} + v\frac{\partial T}{\partial y} = \left(\alpha\frac{\partial^2 T}{\partial y^2} - \frac{1}{k}\frac{\partial q_r}{\partial y}\right). \quad (88)$$

with initial conditions

$$u(x, y) = v(x, y) = 0, T(x, y) = T_\infty,\ t < 0, \quad (89)$$

The boundary conditions for $t \geq 0$

$$u(x, 0) = v(x, 0) = 0, u(x, \infty) = U_e = ax,\ a > 0,$$
$$Tx, \infty = T_\infty, T(x, 0) = T_w(x)bx^n, b > 0, n \geq 0 \quad (90)$$

The corresponding transformations used are

$$\eta=\left(\frac{a\rho}{\mu_\infty}\right)^{\frac{1}{2}}y\xi^{-\frac{1}{2}},\ \xi=1-e^{-t^*}, \tag{91}$$
$$t^*=at,a>0,U(x,y,t)=axf', \tag{92}$$
$$v(x,y,t)=-\left(\frac{a\mu_\infty}{\rho}\right)^{\frac{1}{2}}\xi^{\frac{1}{2}}f(\eta,\xi), \tag{93}$$
$$T(x,y,t)=T_\infty+(T_w-T_\infty)\theta(\eta,\xi), \tag{94}$$
$$Pr=\frac{\mu_\infty}{\rho\alpha},\lambda=\frac{Gr_x}{Re_x^2}, \tag{95}$$
$$Gr_x=g\beta(T_w-T_\infty)\frac{x^3\rho^2}{\mu_\infty^2}, \tag{96}$$
$$Re_x\frac{ax^2\rho}{\mu_\infty}, \tag{97}$$

Using equation (91)-(97) in equations (86)-(88) together with boundary conditions equations (90) we get

$$\begin{aligned}&(1+\sigma\theta)f'''+\sigma\theta'f''+\frac{1}{2}\eta(1-\xi)f''\\&\quad+\xi ff''+\xi(1-(f')^2)+ \qquad (98)\\&\quad+\lambda\theta\xi+\gamma\xi(1-(1+\sigma\theta)f')+\Delta\xi(1-(f')^2)\\&\quad=\xi(1-\xi)\frac{\partial f'}{\partial\xi}, \qquad (99)\end{aligned}$$

$$\begin{aligned}&\frac{1}{Pr}\theta''-R\xi(\theta-1)+\frac{1}{2}\eta(1-\xi)\theta'+\xi(f\theta'-nf'\theta)\\&\quad=\xi(1-\xi)\frac{\partial\theta}{\partial\xi}, \qquad (100)\end{aligned}$$

where $\gamma=\mu_\infty\epsilon/aK\rho$ is the first order resistance parameter, $\Delta=\left[F_1\epsilon^4Re_x\mu_{infty}/aK\rho\right]^{\frac{1}{2}}$, is the second order parameter,$R=4\alpha I/ka$ is the radiation parameter, $\lambda>0$ for buoyancy assisting flow and $\lambda<0$ for buoyancy opposing flow. The boundary conditions reduce to

$$\begin{aligned}&f(0,\xi)=f'(0,\xi)=0,\theta(0,\infty)=1,\\&f'(\infty,\xi)=1,\theta(\infty,\xi)=0. \qquad (101)\end{aligned}$$

For the case $\xi=0$ and $\sigma=0$ the system admits to the solution

$$\begin{aligned}&f=\eta erfc(\frac{\eta}{2})-\frac{2}{\sqrt{\pi}}\left[1-exp(-\frac{\eta^2}{4})\right],\\&\theta=erfc(Pr^{\frac{1}{2}}\frac{\eta}{2}), \qquad (102)\end{aligned}$$

The spectral relaxation method is applied to the system (99) and (101) and becomes;

$$\begin{aligned}&a_{1,r}U''_{r+1}+a_{2,r}U'_{r+1}+a_{3,r}U_{r+1}\\&\qquad=\xi(1-\xi)\frac{\partial U_{r+1}}{\partial\xi}, \qquad (103)\\&f'_{r+1}=U_{r+1}, \qquad (104)\\&\frac{1}{Pr}\theta''_{r+1}+b_{1,r}\theta'_{r+1}+b_{2,r}\theta_{r+1}\\&\qquad=\xi(1-\xi)\frac{\partial\theta_{r+1}}{\partial\xi}, \qquad (105)\end{aligned}$$

with boundary conditions;

$$\begin{aligned}&\eta=0,\quad f_{r+1}=f_w,\\&U_{r+1}=\left(1+\frac{1}{\beta}\right)S_fU'_{r+1},\quad\theta_{r+1}=1+S_T\theta'_{r+1},\\&\eta\to\infty,U_{r+1}\to0,\quad\theta_{r+1}\to0. \qquad (106)\end{aligned}$$

where

$$\begin{aligned}&a_{1,r}=1+\sigma\theta_r,a_{2,r}=\sigma\theta'_r+\frac{1}{2}\eta(1-\xi)+\xi f_r,\\&a_{3,r}=-\gamma\xi(1+\sigma\theta_r), \qquad (107)\\&a_{4,r}=\xi(\gamma+\lambda\theta_r)+(1-U_r^2)(\xi+\Delta\xi), \qquad (108)\\&b_{1,r}=\frac{1}{2}\eta(1-\xi)+\xi f_r,\\&b_{2,r}=\xi(R-nU_r),\ b_{3,r}=R\xi. \qquad (109)\end{aligned}$$

The initial approximations for solving the equations (99) - (101) are obtained by setting $\xi=0$.

$$f_0=1-\eta e^{(-\eta)}-e^{(-\eta)},\theta_0=e^{-\eta}, \tag{110}$$

The iterative schemes (99) - (101) can be solved iteratively for u_{r+1} when $r=0,1,2\ldots$, the solution for u_{r+1} is used to solve for f_{r+1}. To solve the equations we use the Chebyshev spectral method in the $\eta-$ direction and use the implicit finite difference method in the $\xi-$direction. The finite difference scheme is applied with centering about the midpoint halfway between ξ^{n+1} and ξ^n, which is defined as $\xi^{n+\frac{1}{2}}=(\xi^{n+1}+\xi^n)/2$. The derivatives with respect to η are defined in terms of the Chebyshev differentiation matrices. Using the centering about $\xi^{n+\frac{1}{2}}$ to any function, for example $f(\eta,\xi)$ and its corresponding derivative we get,

$$\begin{aligned}&f(\eta_j,\xi^{n+\frac{1}{2}})=f_j^{n+\frac{1}{2}}=\frac{f_j^{n+1}+f_j^n}{2},\\&\left(\frac{\partial f}{\partial\xi}\right)^{n+\frac{1}{2}}=\frac{f_j^{n+1}-f_j^n}{\Delta\xi}. \qquad (111)\end{aligned}$$

Writing the system (99) - (101) in terms of the differentiation matrix we obtain,

$$\begin{aligned}&\left[a_{1,r}\mathbf{D}^2+a_{2,r}\mathbf{D}+\mathbf{a}_{3,r}\right]U_{r+1}+\mathbf{a}_{4,r}\\&\qquad=\xi(1-\xi)\frac{\partial U_{r+1}}{\partial\xi}, \qquad (112)\\&\mathbf{D}f_{r+1}=U_{r+1},f_{r+1}(\eta N_x,\xi)=f_w \qquad (113)\\&\left[\frac{1}{Pr}\mathbf{D}^2+b_{1,r}\mathbf{D}+\mathbf{b}_{2,r}\right]\theta_{r+1}+\mathbf{b}_{3,r}\\&\qquad=\xi(1-\xi)\frac{\partial\theta_{r+1}}{\partial\xi}, \qquad (114)\end{aligned}$$

with boundary conditions;

$$\begin{aligned}&U_{r+1}(\eta N_x,\xi)=\left(1+\frac{1}{\beta}\right)S_fU'_{r+1}(\eta N_x,\xi),\\&\theta_{r+1}(\eta N_x,\xi)=1+S_T\theta'_{r+1}(\eta N_x,\xi),\\&U_{r+1}(\eta_0,\xi)\to0,\quad\theta_{r+1}(\eta_0,\xi)\to0. \qquad (115)\end{aligned}$$

We now apply the finite difference scheme on (112) - (115) in the $\xi-$direction with centering about the mid-point $\xi^{n+\frac{1}{2}}$ to get,

$$\mathbf{A}_1 U_{r+1}^{n+1} = \mathbf{B}_1 U_{r+1}^{n} + \mathbf{K}_1, \tag{116}$$

subject to

$$U_{r+1}(\eta_0, \xi^n) = (1+\frac{1}{\beta})S_f U'_{r+1}(\eta_0, \xi^n),$$
$$U_{r+1}(\eta_{N_x}, \xi^n) \to 0,\ n = 0,1,2,\dots,N_t \tag{117}$$
$$U_{\eta_j,0} = \text{erfc}\left(\frac{\eta_j}{2}\right),\ j = 0,1,2,\dots,N_x. \tag{118}$$

where

$$\mathbf{A}_1 = \frac{1}{2}\left((\mathbf{a}_{1,r})^{n+\frac{1}{2}}\mathbf{D}^2 + (\mathbf{a}_{2,r})^{n+\frac{1}{2}}\mathbf{D} + (\mathbf{a}_{3,r})^{n+\frac{1}{2}}\right) - \frac{\xi^{n+\frac{1}{2}}(1-\xi^{n+\frac{1}{2}})}{\Delta\xi}, \tag{119}$$

$$\mathbf{B}_1 = -\frac{1}{2}\left((\mathbf{a}_{1,r})^{n+\frac{1}{2}}\mathbf{D}^2 + (\mathbf{a}_{2,r})^{n+\frac{1}{2}}\mathbf{D} + (\mathbf{a}_{3,r})^{n+\frac{1}{2}}\right) - \frac{\xi^{n+\frac{1}{2}}(1-\xi^{n+\frac{1}{2}})}{\Delta\xi}, \tag{120}$$

$$\mathbf{K}_1 = -\mathbf{a}_{4,r}^{n+\frac{1}{2}}, \tag{121}$$

$$\mathbf{A}F_{r+1}^{n+1} = U_{r+1}^{n}, \tag{122}$$

subject to

$$F_{r+1}(\eta N_x, \xi) = f_w. \tag{123}$$

$$\mathbf{A}_2\Theta_{r+1}^{n+1} = \mathbf{B}_2\Theta_{r+1}^{n} + \mathbf{K}_2, \tag{124}$$

subject to

$$\Theta_{r+1}(\eta N_x, \xi) = 1 + S_T\Theta'_{r+1}(\eta N_x, \xi),$$
$$\Theta_{r+1}(\eta_0, \xi) \to 0, \tag{125}$$

where

$$\mathbf{A}_2 = \frac{1}{2}\left(\frac{1}{Pr}\mathbf{D}^2 + (\mathbf{b}_{1,r})^{n+\frac{1}{2}}\mathbf{D} + \mathbf{b}_{2,r})^{n+\frac{1}{2}}\right) - \frac{\xi^{n+\frac{1}{2}}(1-\xi^{n+\frac{1}{2}})}{\Delta\xi}, \tag{126}$$

$$\mathbf{B}_2 = -\frac{1}{2}\left(\frac{1}{Pr}\mathbf{D}^2 + (\mathbf{b}_{1,r})^{n+\frac{1}{2}}\mathbf{D} + \mathbf{b}_{2,r})^{n+\frac{1}{2}}\right) - \frac{\xi^{n+\frac{1}{2}}(1-\xi^{n+\frac{1}{2}})}{\Delta\xi}, \tag{127}$$

$$\mathbf{K}_2 = \mathbf{b}_{3,r}^{n+\frac{1}{2}}, \tag{128}$$

The boundary conditions in (118) are imposed on the first and last rows of equation (116), those in equation (123) are imposed on the last row of equation (122) and those in equation (125) are imposed in the first and last rows of equation (124).

6. Example 4: Double diffusive mixed convection flow from a vertical exponentially stretching surface in the presence of viscous dissipation

In this section we make use of the example from Patil et al. [26] mixed convection from a vertical stretching surface and viscous dissipation. The governing equation is given by;

$$\frac{\partial u}{\partial x} + \frac{\partial v}{\partial y} = 0, \tag{129}$$

$$u\frac{\partial u}{\partial x} + v\frac{\partial u}{\partial y} = U_e\frac{dU_e}{dx} + \nu\frac{\partial^2 u}{\partial y^2} + g\beta(T-T_\infty) + g\beta^*(C-C_\infty), \tag{130}$$

$$u\frac{\partial T}{\partial x} + v\frac{\partial T}{\partial y} = \frac{\nu}{Pr}\frac{\partial^2 T}{\partial y^2} + \frac{\nu}{C_p}\left(\frac{\partial u}{\partial y}\right)^2 + Q\frac{T-T_\infty}{\rho C_p}, \tag{131}$$

$$u\frac{\partial C}{\partial x} + v\frac{\partial C}{\partial y} = \frac{\nu}{Sc}\frac{\partial^2 C}{\partial y^2}, \tag{132}$$

In the equations, B is the magnetic field strength, β and β^* are the thermal and concentration coefficients of volumetric expansion respectively, σ is the electrical conductivity. The boundary conditions are given as;

$$y = 0 :,\ u = U_w(x),\ v = v_w,$$
$$T = T_w, = T_\infty + (T_{w0} - T_\infty)exp(\frac{2x}{L}),$$
$$C = C_w, = C_\infty + (C_{w0} - C_\infty)exp(\frac{2x}{L}),$$
$$y \to \infty :,\ u \to U_e(x),\ T \to T_\infty, C \to C_\infty. \tag{133}$$

Using the following dimensionless variables,

$$\xi = \frac{x}{L},\ \eta = \frac{U_0}{\nu x}exp(\frac{x}{2L})y, \tag{134}$$
$$\psi(x,y) = (\nu U_0 x)^{\frac{1}{2}}exp(\frac{x}{2L})f(\xi,\eta), \tag{135}$$
$$T - T_\infty = (T_w - T_\infty)G(\xi,\eta), \tag{136}$$
$$T - T_\infty = (T_w - T_\infty)e^{(\frac{x}{2L})}, \tag{137}$$
$$C - C_\infty = (C_w - C_\infty)H(\xi,\eta), \tag{138}$$
$$C - C_\infty = (C_w - C_\infty)e^{(\frac{x}{2L})}, \tag{139}$$
$$u = \frac{\partial\psi}{\partial y},\ v = -\frac{\partial\psi}{\partial x},\ u = U_0 e^{(\frac{x}{L})}f', \tag{140}$$
$$v = -(\frac{\nu U_0}{x})^{\frac{1}{2}}e^{(\frac{x}{2L})}\left((1+\xi)\frac{f}{2} + \xi\frac{\partial f}{\partial\xi} + \frac{\eta}{2}\frac{\partial f}{\partial\eta}\right) \tag{141}$$

The following system of partial differential equations is obtained,

$$f''' + \frac{1}{2}(1+\xi)ff'' - \xi f'^2 + \xi Ri(G+NH) + \xi\epsilon^2 = 4\xi\left(f'\frac{\partial f'}{\partial\xi} - f''\frac{\partial f}{\partial\xi}\right), \tag{142}$$

$$G'' + \frac{Pr}{2}(1+\xi)fG' - 2Pr\xi f'G + PrEc(f'')^2 + Re\Gamma Pr\xi G = Pr\xi\left(f'\frac{\partial\theta}{\partial\xi} - \theta'\frac{\partial f}{\partial\xi}\right) \quad (143)$$

$$H'' + \frac{Sc}{2}(1+\xi)fH' - 2Sc\xi f'H = Sc\xi\left(f'\frac{\partial H}{\partial\xi} - H'\frac{\partial f}{\partial\xi}\right), \quad (144)$$

with boundary conditions;

$$f'(\xi,0)=0,\ f(\xi,0)=0,\ \theta(\xi,0)=1, H(\xi,0)=1,$$
$$f'(\xi,\infty)=1,\ \theta(\xi,\infty)=0, H(\xi,\infty)=0. \quad (145)$$

In the above equations, for the case $\xi = 0$, the equations do not reduce to those of Magyari and Keller [33], Bidin and Nazar [29] and Mukhopadhyay [30] as mentioned in Patil et al. [26], but rather to those of Watanabe and Pop [27]. The spectral relaxation method is applied to the system (142) and (145) and becomes;

$$U''_{r+1} + a_{1,r}U'_{r+1} + a_{2,r} = a_{3,r}\frac{\partial U_{r+1}}{\partial\xi}, \quad (146)$$
$$U_{r+1}(\xi,0)=1,\ U_{r+1}(\xi,\infty)=0, \quad (147)$$
$$f'_{r+1} = U_{r+1},\ f_{r+1}(\xi,0)=0, \quad (148)$$
$$G''_{r+1} + b_{1,r}G'_{r+1} + b_{2,r}G_{r+1} + b_{3,r} = b_{4,r}\frac{\partial G_{r+1}}{\partial\xi}, \quad (149)$$
$$G_{r+1}(\xi,0)=1,\ G_{r+1}(\xi,\infty)=0, \quad (150)$$
$$H''_{r+1} + c_{1,r}H'_{r+1} + c_{2,r}H_{r+1} = c_{3,r}\frac{\partial H_{r+1}}{\partial\xi}, \quad (151)$$
$$H_{r+1}(\xi,0)=1,\ H_{r+1}(\xi,\infty)=0, \quad (152)$$

where

$$a_{1,r} = \frac{1}{2}(1+\xi)f_r + \xi\frac{\partial f_r}{\partial\xi}, \quad (153)$$
$$a_{2,r} = -\xi U_r^2 + \xi Ri(G_r + NH_r) + \xi\epsilon^2, \quad (154)$$
$$a_{3,r} = \xi U_r, \quad (155)$$
$$b_{1,r} = \frac{Pr}{2}(1+\xi)f_r + Pr\xi\frac{\partial f_r}{\partial\xi}, \quad (156)$$
$$b_{2,r} = -\xi Pr(2U_r - Re\Gamma), \quad (157)$$
$$b_{3,r} = PrEc(U'_r)^2, b_{4,r} = \xi PrU_r, \quad (158)$$
$$c_{1,r} = \frac{Sc}{2}(1+\xi)f_r + Sc\xi\frac{\partial f_r}{\partial\xi}, \quad (159)$$
$$c_{2,r} = -2Sc\xi U_r, \quad (160)$$
$$c_{3,r} = \xi ScU_r, \quad (161)$$

We now apply the finite difference scheme on (146) - (152) in the $\xi-$direction with centering about the midpoint $\xi^{n+\frac{1}{2}}$ to obtain,

$$\mathbf{A}_1U_{r+1}^{n+1} = \mathbf{B}_1U_{r+1}^{n} + \mathbf{K}_1, \quad (162)$$

subject to

$$U_{r+1}(\eta N_x,\xi)=1,\ U_{r+1}(\eta_0,\xi)\to 0, \quad (163)$$

where

$$\mathbf{A}_1 = \frac{1}{2}\left(\mathbf{D}^2 + (\mathbf{a}_{1,r})^{n+\frac{1}{2}}\mathbf{D}\right) - \frac{(\mathbf{a}_{3,r})^{n+\frac{1}{2}}}{\Delta\xi}, \quad (164)$$
$$\mathbf{B}_1 = -\frac{1}{2}\left(\mathbf{D}^2 + (\mathbf{a}_{1,r})^{n+\frac{1}{2}}\mathbf{D}\right) - \frac{(\mathbf{a}_{3,r})^{n+\frac{1}{2}}}{\Delta\xi}, \quad (165)$$
$$\mathbf{K}_1 = -\mathbf{a}_{2,r}^{n+\frac{1}{2}}, \quad (166)$$

$$\mathbf{A}F_{r+1}^{n+1} = U_{r+1}^{n}, \quad (167)$$

subject to

$$F_{r+1}(\eta N_x,\xi)=0. \quad (168)$$

$$\mathbf{A}_2\theta_{r+1}^{n+1} = \mathbf{B}_2\theta_{r+1}^{n} + \mathbf{K}_2, \quad (169)$$

subject to

$$\theta_{r+1}(\eta N_x,\xi)=1,\ \theta_{r+1}(\eta_0,\xi)\to 0, \quad (170)$$

where

$$\mathbf{A}_2 = \frac{1}{2}\left(\mathbf{D}^2 + (\mathbf{b}_{1,r})^{n+\frac{1}{2}}\mathbf{D} + \mathbf{b}_{2,r})^{n+\frac{1}{2}}\right) - \frac{(\mathbf{b}_{4,r})^{n+\frac{1}{2}}}{\Delta\xi}, \quad (171)$$
$$\mathbf{B}_2 = -\frac{1}{2}\left(\mathbf{D}^2 + (\mathbf{b}_{1,r})^{n+\frac{1}{2}}\mathbf{D} + \mathbf{b}_{2,r})^{n+\frac{1}{2}}\right) - \frac{(\mathbf{b}_{4,r})^{n+\frac{1}{2}}}{\Delta\xi}, \quad (172)$$
$$\mathbf{K}_1 = -\mathbf{b}_{3,r}^{n+\frac{1}{2}}, \quad (173)$$

$$\mathbf{A}_3H_{r+1}^{n+1} = \mathbf{B}_3H_{r+1}^{n} + \mathbf{K}_3, \quad (174)$$

subject to

$$H_{r+1}(\eta N_x,\xi)=1,\ H_{r+1}(\eta_0,\xi)\to 0, \quad (175)$$

where

$$\mathbf{A}_3 = \frac{1}{2}\left(\mathbf{D}^2 + (\mathbf{c}_{1,r})^{n+\frac{1}{2}}\mathbf{D} + (\mathbf{c}_{2,r})^{n+\frac{1}{2}}\right) - \frac{(\mathbf{c}_{3,r})^{n+\frac{1}{2}}}{\Delta\xi}, \quad (176)$$
$$\mathbf{B}_3 = -\frac{1}{2}\left(\mathbf{D}^2 + (\mathbf{c}_{1,r})^{n+\frac{1}{2}}\mathbf{D} + (\mathbf{c}_{2,r})^{n+\frac{1}{2}}\right) - \frac{(\mathbf{c}_{3,r})^{n+\frac{1}{2}}}{\Delta\xi}, \quad (177)$$
$$\mathbf{K}_3 = \mathbf{0}. \quad (178)$$

7. Results and discussion

The spectral relaxation method (SRM) for solving boundary value problems is presented in this paper, four examples of boundary value problems were presented in the previous sections. In this section we discuss the results for all numerical examples considered. The method depends on the length of the governing domain $(b-a)$ and the number of collocation points N sometimes referred to as grid points. The domain of the given numerical examples are defined on $[0,\infty)$, to implement the SRM scheme we need to find the appropriate finite value η_∞ which is large enough to approximate infinity for the given example. We start with an initial guess and solve the SRM scheme over $[0,\eta_\infty]$ so we obtain solutions for the fluid flow functions $f(\eta), g(\eta), h(\eta)$ for example 1, $f(\eta), \theta(\eta), \phi(\eta)$ for example 2, $f(\eta), \theta(\eta)$ for example 3 and $f(\eta), \theta(\eta), \phi(\eta)$ for example 4. The derivatives of these functions at $\eta = 0$ are also computed to obtain the important values $f''(0)$ (skin friction coefficient), $-\theta'(0)$ (heat transfer coefficient) and $-\phi'(0)$ (mass transfer coefficient).

The numerical scheme is implemented by increasing the value of η_∞ by one and the solution process repeated until the difference in values of $f''(0), -\theta'(0)$ and $-\phi'(0)$ between current and previous solution is less that a specified tolerance level. If the optimal value of η_∞ is identified for a particular set governing constants, the minimum number of grid points is obtained using a similar process. Starting with a small value of N, say $N = 40$, the value of N is increased by 10 and the solution is solved until the results do not change within the specified tolerance level. The accuracy of the SRM results presented in this Chapter validated by comparison with those previously published in the literature. The results were compared against the MATLAB `bvp4c` solver. The comparisons show a good agreement. It is also observed that the error decrease at every iteration showing the convergence and stability of the solutions produced by the SRM.

Table 1: Comparison of the values of $f''(0)$ obtained by SRM against those of Ece [24] and bvp4c for example 1 for $\epsilon = M = 0$, 90 iterations and $\eta_\infty = 10$

Pr	$f''(0)$**Ece [24]**	$f''(0)$ **bvp4c**	$f''(0)$ **SRM**
1	0.68150212	0.68147996	0.68147995
10	0.43327726	0.43327802	0.43327802

In Table 1, the SRM results for skin friction coefficient agrees with the results of Ece [24] and MATLAB `bvp4c` to six decimal places, this shows the accuracy of the SRM for example 1.

Table 2: Comparison of the values of $f''(0)$ obtained by SRM against those of Awad [25] and bvp4c for example 2 with $Sc = 0.2, N_1 = 0.5, D_f = 0.1, S_r = 0.3, Pr = 0.71, \lambda = 1$. 90 iterations and $\eta_\infty = 12$

Λ	$f''(0)$ **Awad [25]**	$f''(0)$ **bvp4c**	$f''(0)$ **SRM**
0.3	1.0160906	1.0160906	1.0160906
0.5	0.9748755	0.9748755	0.9748755

In Table 2, the SRM results for skin friction coefficient agrees with the results of Awad [25] and MATLAB `bvp4c` to six decimal places, this shows the accuracy of the SRM for example 2.

Table 3: Comparison of the values of $-\theta'(0)$ obtained by SRM against those of Hassanien and Al-Arabi. [31] and QLM for example 3 with $\gamma = \Lambda = \sigma = R = \xi = 0, n = 0, Pr = 0.7$ 90 iterations and $\eta_\infty = 10$

ξ	$-\theta'(0)$ **[31]**	$-\theta'(0)$ **QLM**	$-\theta'(0)$ **SRM**
0	0.47204	0.472035	0.472035
0.5	0.46347	0.463471	0.463471

In Table 3, the SRM results for the heat transfer coefficient agrees with the results of Hassanien and Al-Arabi. [31] and QLM to six decimal places, this shows the accuracy of the SRM for example 3.

Table 4: Comparison of the values of $-\theta'(0)$ obtained by SRM against those of Watanabe [27] and bvp4c for example 4 with $M = N = 0, Sc = 1, Pr = 1$.

ξ	$-\theta'(0)$ **[27]**	$-\theta'(0)$ **QLM**	$-\theta'(0)$ **SRM**
0	0.33026	0.33025734	0.33025734
0.5	0.40280	0.40279671	0.40279671

In Table 4, the SRM results for the heat transfer coefficient agrees with the results of Watanabe [27] and QLM to eight decimal places, this shows the accuracy of the SRM for example 4.

DOI: 10.37394/23202.2022.21.22

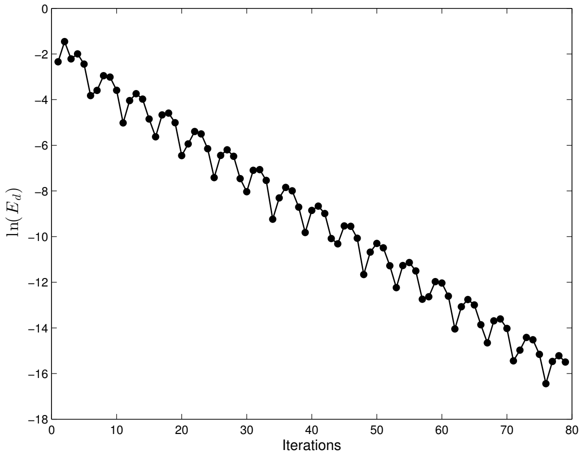

(a)

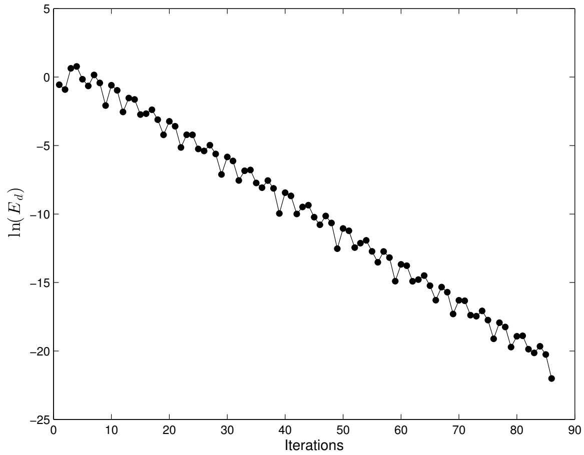

(b)

Fig. 1: Logarithm of the SRM decoupling error for (a) Example 1 and (b) Example 2.

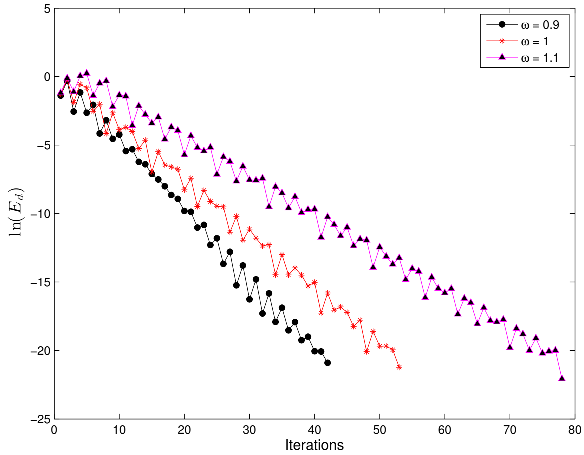

(a)

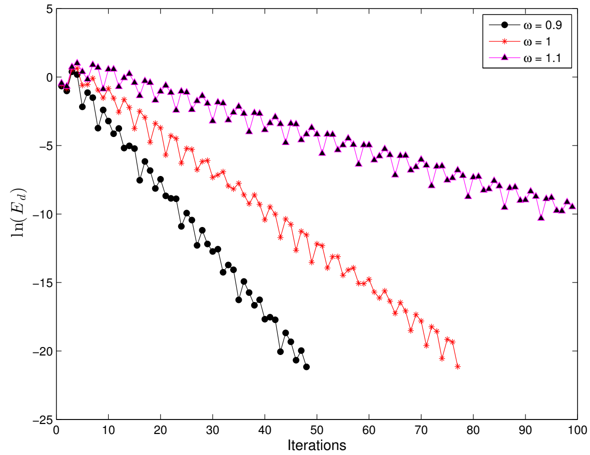

(b)

Fig. 2: Logarithm of the SRM with SOR decoupling error for (a) Example 1 and (b) Example 2.

In Figure 1, the logarithm of the SRM decoupling error decreases with increasing iteration showing the rapid convergence and stability of the SRM for (a) Example 1 and (b) Example 2. This is the standard SRM without the successive over-relaxation (SOR). Convergence is also affected by the parameter values. These affect in many different ways, they can slow convergence or cause complete divergence. When certain parameters assume higher or even lower values, the method might require more iterations to converge. In the graph, the larger the negative values on the vertical axis, the smaller the error. The SRM requires the use of the SOR to control its convergence. In these two examples, the SRM requires more than 70 iterations. Example 1 required more iterations to achieve a larger error than that of example 2 that required less number of iterations.

The convergence of the SRM can be controlled by using the successive over-relaxation (SOR) method. This is achieved by varying the relaxation parameter ω. In Figure 2, when $\omega = 0.9$ the SRM converges faster and when $\omega = 1.1$ slows down convergence. The value $\omega = 1$ corresponds to the standard SRM (without SOR). The application of the successive over-relaxation was consistent in both examples 1 and 2. The effect of over-relaxation was is more enhanced in example 2 than in example 1. This is caused by the parameter values in each of these examples. The SRM will require a smaller value of ω to achieve a faster convergence. For values of $\omega > 1$ (purple line) more iterations are required. For $\omega = 1$ (Red line), similar to Figure 1. $\omega < 1$ (black line), the number of iterations is reduced significantly.

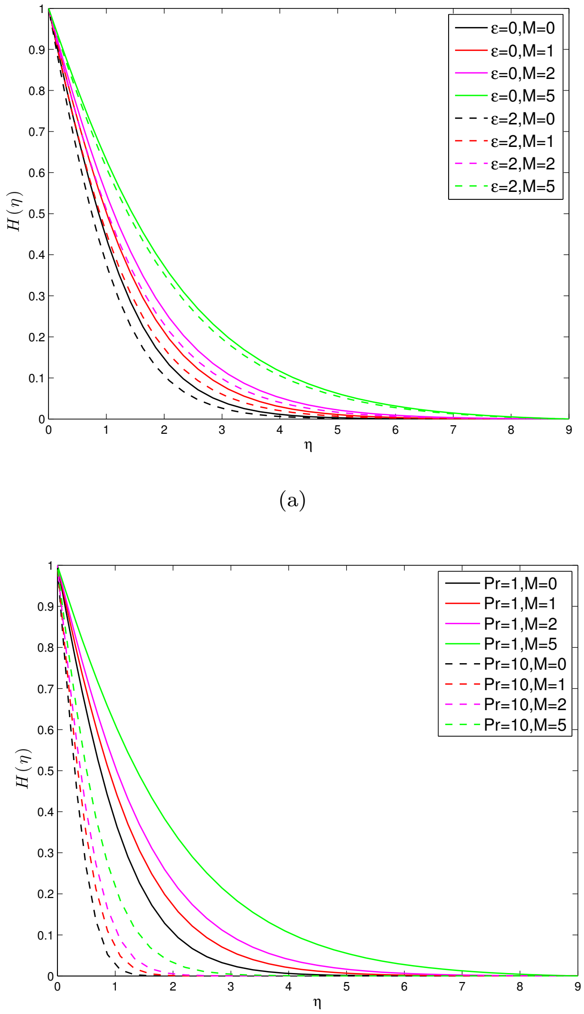

(a)

(b)

Fig. 3: Variation of (a) spin parameter and (b) magnetic parameter on temperature profiles for Example 1

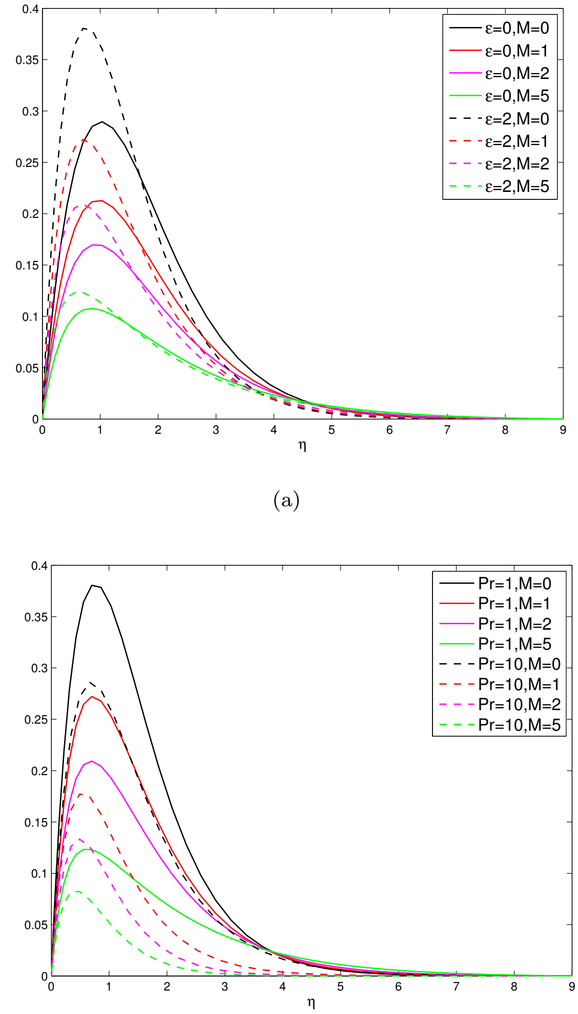

(a)

(b)

Fig. 4: Variation of (a) spin parameter and (b) magnetic parameter on velocity profiles for Example 1

Figure 3 shows the variation the spin parameter ϵ and Prandtl number Pr in the presence of the magnetic field on temperature profiles. It is observed that increasing both the spin parameter and Prandtl number reduce temperature profiles. Increasing the spin parameter has an effect of reducing the velocity profiles, this is because the direction of rotation is at right angles with the direction of fluid flow. The reduction in fluid velocity in the direction of flow cause reduction in heat transfer, thereby reducing temperature profiles. Increasing the magnetic parameter will have the same effect of reducing velocity profiles and also reducing heat transfer. Increasing the Prandtl number has an effect of reducing thermal diffusivity as shown in this figure. These results are consistent with those reported by Ece [24]. This confirms that the SRM is accurate and can also be used as an alternative method for solving

Figure 4 shows the variation the spin parameter ϵ and Prandtl number Pr in the presence of the magnetic field on velocity profiles. It is observed that increasing the spin parameter result in the decrease in velocity profiles and increasing the Prandtl number reduce velocity profiles. The increase in spin parameter result in the decrease in velocity profiles, this caused by the spin velocity which is tangential to the velocity of the fluid flow. This has a dragging effect on the fluid flow. The Increase in the magnetic parameter result in the retardation of fluid flow as it is directed perpendicular to the fluid flow. Increasing the Prandtl number result in the direct increase of momentum diffusivity. This agrees with the result reported in Ece [24]. This shows that the SRM is accurate and can be used to solve boundary value problems in fluid flow.

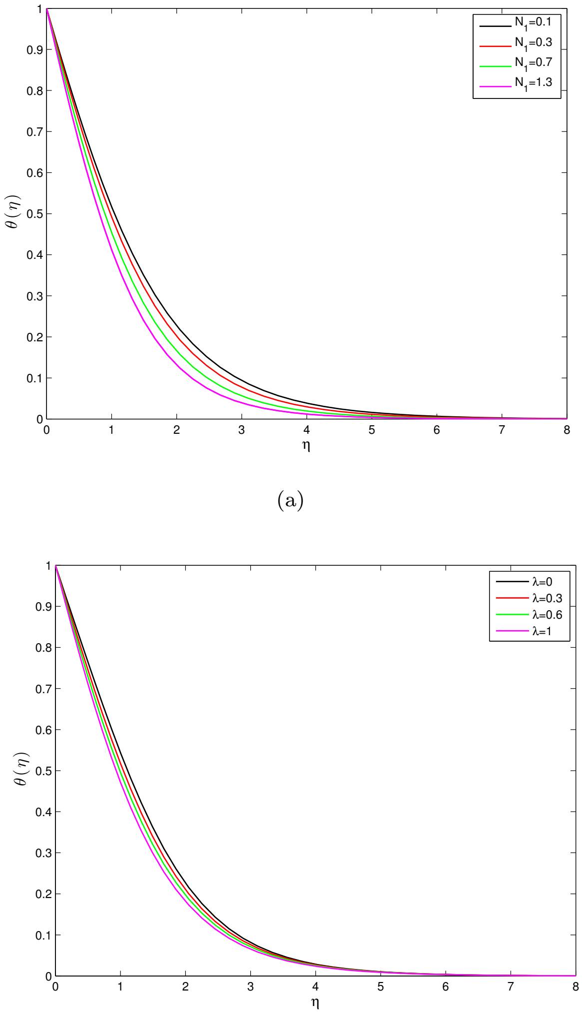

(a)

(b)

Fig. 5: Variation of (a) concentration buoyancy parameter and (b) power-law index on tempearture profiles for Example 2

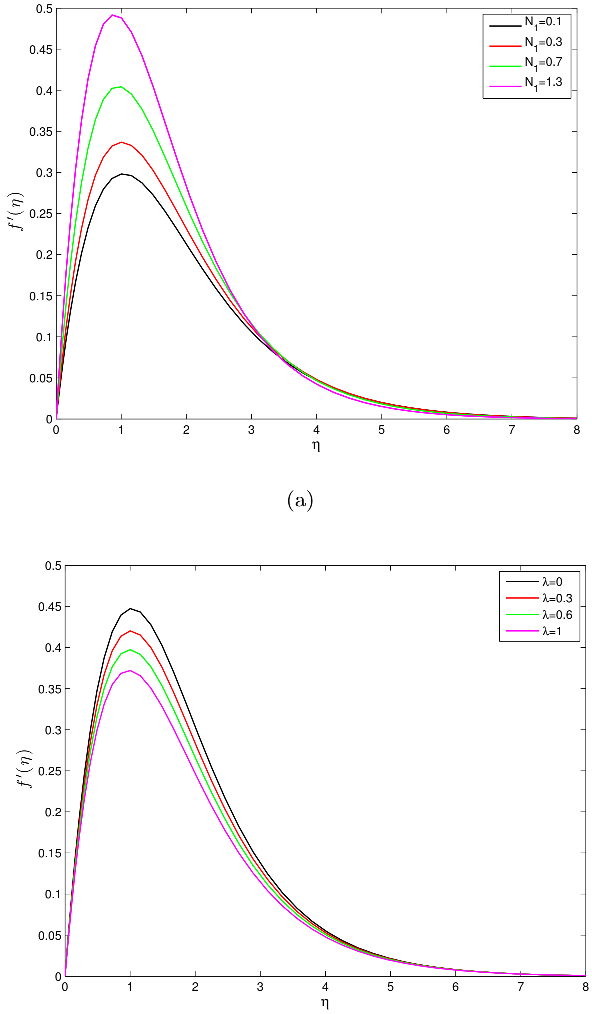

(a)

(b)

Fig. 6: Variation of (a) concentration buoyancy parameter and (b) power-law index on velocity profiles for Example 2

Figure 5 shows the variation of concentration buoyancy parameter N_1 and power-law index λ on temperature profiles. Increasing both the concentration buoyancy parameter and power-law index result in the decrease in temperature profiles. Increasing the concentration buoyancy parameter result in the decrease in temperature profiles, the high buoyancy aids fluid motion. The presence of the solute cause a decrease in temperature profiles as shown in Figure 5 (a). Also increasing the power-law index result in the decrease in temperature profiles as shown in Figure 5 (b). The results are consistent with those of Awad et. al [25].

Figure 6 shows the effect of increasing the buoyancy parameter N_1 and power-law index λ.Increasing the buoyancy parameter result in the increase in velocity profiles, concentration buoyancy tend to aid fluid motion, the solute is pushed by the buoyancy force and increase fluid motion as shown in 6 (a). Increase in power-law index result in the decrease in velocity profiles as shown in Figure 6 (b). These results agree with those of Awad et. al [25].

DOI: 10.37394/23202.2022.21.22

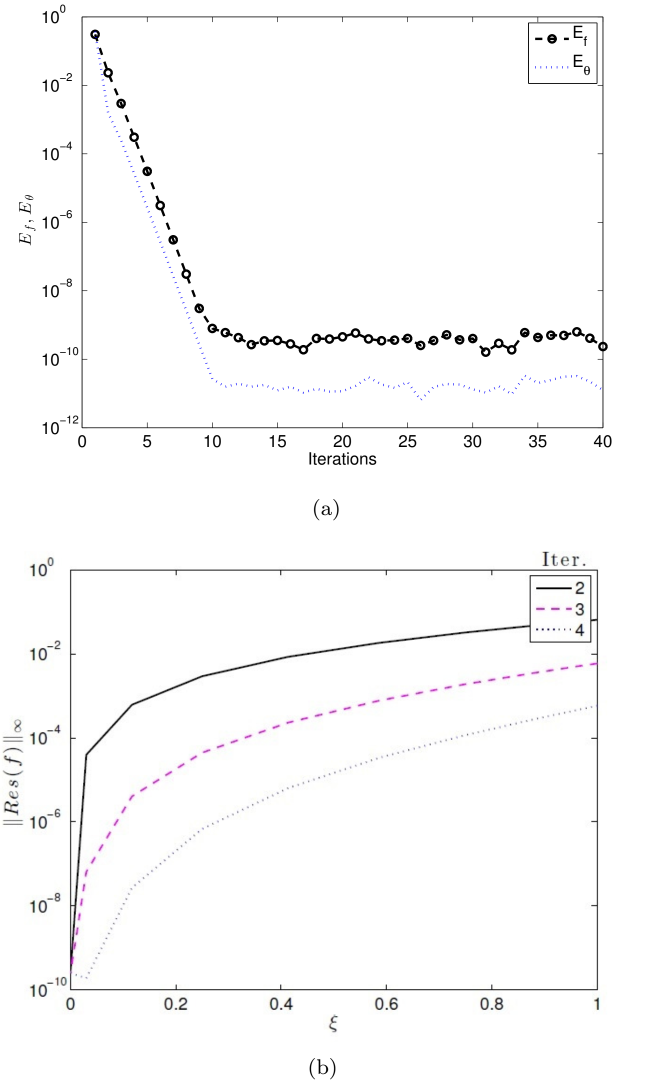

Fig. 7: (a) Convergence graph for $f(\eta,\xi), \theta(\eta,\xi)$, (b) Residual graph for $f(\eta,\xi)$ for Example 3

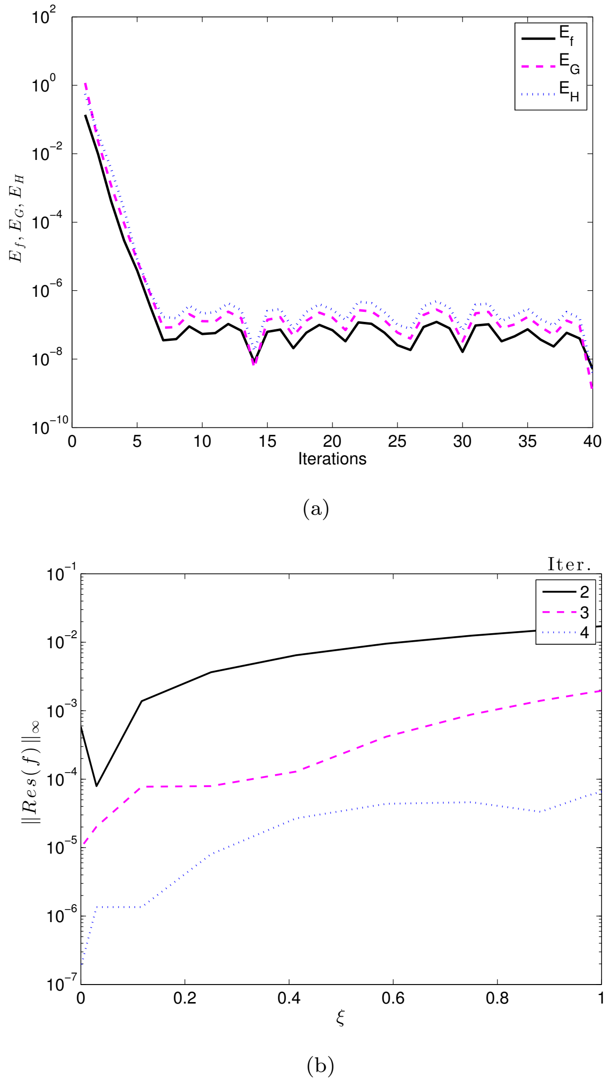

Fig. 8: (a) Convergence graph for $f(\eta,\xi), G(\eta,\xi), H(\eta,\xi)$, (b) Residual graph for $f(\eta,\xi)$ for Example 4

Figure 7 indicates the error graphs for example 3. Figure 7 (a) shows the rapid convergence of the SRM after ten iterations, thereafter it is observed that the SRM is stable. The stability of the SRM was observed for both momentum and thermal equations. The errors are as small as the order of 10^{-12}. In Figure 7 (b) we observe the increase in the error as ξ increase. The error decrease with increasing iterations. The most important result is the effect of the time dimension ξ on error propagation.

The accuracy of the SRM for example 4 is shown in Figure 8 (a) and Figure 8 (b), showing the reduction of the error with increasing number of iterations. It is observed that there is rapid convergence of the SRM in about 10 iterations, the error being of the order of 10^{-11}. The stability of the SRM is shown after 10 iterations, the variation of the error does not change much showing the accuracy of the method. Figure 8 (b) shows the plot of residual error of the function $f(\eta,\xi)$ against ξ with increasing iteration. It is observed that the rate of increasing the residual error is almost linear and is minimum at $\xi = 0$. The error increases sharply and reach a level where it is almost constant. We further observe that the error is small after two iterations in the entire range of the values of ξ. The small size of the residual error indicate the accuracy of the method.

Table 5: Heat transfer coefficient $-\theta'(0,\xi)$ for various values of ξ computed using SRM for example 3.

$\xi/\Delta\xi$	0.004	0.001	0.0005
0.1	0.475693	0.475694	0.475694
0.3	0.483407	0.483407	0.483407
0.5	0.491688	0.491688	0.491688
0.7	0.500488	0.500488	0.500488
CPU Time	1.64	5.98	11.79

Tables 5 and 6 show the numerical values of values of the heat transfer coefficient $-\theta'(0)$ for different values of $\Delta\xi$, computed using the SRM and the QLM respectively for equation (99)-(101).The total computational time to execute the integration is also shown. The computation was done using the same number of collocation points N_x and η_∞. Reducing the step size $\Delta\xi$ improves the accuracy of the results until they are consistent to within six decimal places.

Table 6: Heat transfer coefficient $-\theta'(0,\xi)$ for various values of ξ computed using QLM for example 3.

$\xi/\Delta\xi$	0.004	0.001	0.0005
0.1	0.465195	0.467389	0.467922
0.3	0.459767	0.461433	0.461856
0.5	0.455776	0.457277	0.456466
0.7	0.457627	0.456340	0.500488
CPU Time	5.16	20.1	40.5

The SRM takes less computational time than the QLM, we observe that the SRM converge more rapidly than the QLM when the step size is reduced. Full convergence to six decimal digits is arrived when $\Delta\xi = 0.001$ in the SRM compared to the QLM which showed convergence at $\Delta\xi = 0.0002$.

Table 7: Skin friction coefficient $f''(0,\xi)$ for various values of ξ computed using SRM for example 4.

$\xi/\Delta\xi$	0.004	0.001	0.0005
0.1	0.287824	0.287832	0.287832
0.2	0.249535	0.249542	0.249542
0.3	0.216382	0.216387	0.216387
0.4	0.187672	0.187677	0.187677
CPU Time	4.03	15.8	35.9

Table 8: Skin friction coefficient $f''(0,\xi)$ for various values of ξ computed using QLM for example 4.

$\xi/\Delta\xi$	0.004	0.001	0.0005
0.1	0.286511	0.287828	0.287832
0.2	0.248912	0.249538	0.249542
0.3	0.215822	0.216291	0.216387
0.4	0.186538	0.187482	0.187677
CPU Time	5.16	20.1	40.9

The results shown in Tables 7 and 8 show the accuracy of the SRM, the results for the skin friction coefficient become consistent to six decimal places when $\Delta\xi = 0.001$ compared to the QLM which become consistent at $\Delta\xi = 0.0005$. This shows that the SRM converges more rapidly than the QLM. The computation times shown also reveal that the SRM requires less computation time to execute the integration, these results were also observed in example 3. For further reading, readers are referred to the works of Magagula et al. [33], Motsa et al. [34], Kamwswaran et al. [35], Agbaje and Motsa [36], Shateyi [37] and Motsa and Makukula [38].

8. Conclusion

The objective of this paper was to describe the spectral relaxation method (SRM) and consider different examples in implementing it. Two examples involving ordinary differential equations and two examples involving partial differential equations were considered. The method is easy to implement as compared to finite difference methods such as the Keller-box method. The SRM is a robust and accurate method to solve differential equations and requires less computation time than the quasi-linearization method. The method can be used to solve boundary value problems. The method give results that are accurate in the specified space and time domains. The residual error quickly approaches zero within a few iterations. The method make use of well-known Chebyshev spectral collocation method for discretization. The method has also been improved by considering discretization in both space and time. The challenge in the method is the determination of the appropriate number of collocation points or grid points.

Acknowledgment

I would like to thank the Faculty Research and Innovation Committee (FRIC) of the Central University of Technology, Free State for the sponsorship of this article registration fees, travel and accommodation.

References

[1] M. Tatari, M. Haghighi, A generalized Laguerre spectral collocation method for solving initial-boundary value problems, *Applied Mathematical Modelling*, **38**, 1351-1364, 2014

[2] M. T. Vilhena, L. B. Barichello, J. R. Zabadal, C. F. Segatto, A. V. Cardona, R. P. Pazos, Solutions to the multidimensional linear transport equation by the spectral method, *Progress in Nuclear Energy*, **35**, 275-291, 1999

[3] B. Orel, A. Perne, Chebyshev-Fourier spectral methods for nonperiodic boundary value problems. *Journal of Applied Mathematics*, **2014**, Article ID 572694, 10 pages, **doi**: 10.1155/2014/572694, 2014

[4] F. Fakhar-Izadi, M. Dehghan, Spectral methods for parabolic Volterra integro-differential equations, *Journal of Computation and Applied Mathematics*, **235**, 4032-4046, 2011

[5] R. Moulla, L. Lefevre,B. Maschke, Pseudo-spectral methods for the spatial sympletic reduction of open systems of conservation laws, *Journal of Computational Physics*, **231**, 1272-1292, 2012

[6] G. Makanda, O. D. Makinde, P. Sibanda, Natural convection of viscoelastic fluid from a cone embedded in a porous medium with viscous dissipation, *Mathematical Problems in Engineering*, **2013**, Article ID 934712, 11 pages, **doi**: 10.1155/2013/934712, 2013

[7] S. Motsa, S. Shateyi, A successive linearization method approach to solve Lane-Emdem type of equations, *Mathematical Problems in Engineering*, **2012**, Article ID 280702, 14 pages, **doi**: 10.1155/2012/280702, 2012

[8] S. Motsa, P. Sibanda, A note on the solutions of the Van der Pol and Duffing equations using a linearization method, *Mathematical Problems in Engineering*, **2012**, Article ID 693453, 10 pages, **doi**: 10.1155/2012/693453, 2012

[9] S. S. Motsa, V. M. Magagula, P. Sibanda, A bivarate Chebyshev spectral collocation quasilinearization method for nonlinear evolution parabolic equations, *The Scientific World Journal*, **2014**, Article ID 581987, 13 pages, **doi**: 10.1155/2014/581987, 2014

[10] A. Rashid, M. Abbas, A.I. Ismail, A. A. Md Majid, Numerical solution of the coupled viscous Burgers equations by Chebyshev-Legendre-Legendre pseudo-spectral method, *Applied Mathematics and Computation*, **245**, 372-381, 2014

[11] M. A. Christou, N. C. Papanicolaou, Kawahara solutions in Boussinesq equations using a robust Christov-Galerkin spectral method, *Applied Mathematics and Computation*, **243**, 245-257, 2014

[12] D. Gottlieb, J. S. Hesthaven, Spectral methods for hyperbolic problems. *Journal of Computation and Applied Mathematics*, **128**, 83-131, 2001

[13] D. Gottlieb, S. A. Orszag, *Numerical analysis of spectral methods: Theory and applications*, Capital City Press, Montpelier, Vermont, USA, 1977

[14] R. Jovanovic, S. Kais, F. H. Alharbi, Spectral method for solving the nonlinear Thomas-Fermi equation based on exponential functions, *Journal of Applied Mathematics*, **2014**, Article ID 168568, 8 pages, **doi**: 10.1155/2014/168568, 2014

[15] J. Zhou, The constants in a posteriori error indicator for state-constrained optimal control problems with spectral methods, *Abstracts and Applied Analysis*, **2014**, Article ID 946026, 8 pages, **doi**: 10.1155/2014/946026, 2014

[16] A. Kadem, Analytical solutions for the neutron transport using the spectral methods, *International Journal of Mathematical Science*, **2006**, Article ID 16214, 11 pages, **doi**:10.1155/IJMMS/2006/16214, 2006

[17] W. Wang, C. Xu, Spectral methods based on new formulations of coupled Stokes and Darcy equations, *Journal of Computational Physics*, **257**, 126-142, 2014

[18] I. Kozar ,N. T. Malic, Spectral method in realistic modelling of bridges under moving vehicles, *Engineering Structures*, **50**, 149-157, 2013

[19] C. Pozrikidis, A spectral collocation method with triangular boundary elements, *Engineering Analysis with Boundary Elements*, **30**, 315-324, 2006

[20] P. G. Dlamini, M. Khumalo, S. S. Motsa, A Note on the multi-stage spectral relaxation method for chaos control and synchronization, *International Journal of Nonlinear Sciences and Numerical Simulation*, **15**, 289-298, 2014

[21] S. Shateyi, G. T. Marewo, "Numerical analysis of MHD stagnation point flow of Casson fluid, heat and mass transfer over a stretching sheet" In Balicki, J. (Ed) *Advances in Applied and Pure Mathematics, WSEAS*, *Proceedings of the 7th international conference on finite differences, finite elements, finite volumes, boundary elements (F-and-B'14)*, Gdansk, Poland, 128-132, 2014 **ISBN**: 978-960-474-380-3

[22] S. S. Motsa, Z. G. Makukula, On spectral relaxation method approach for steady Von Karman flow of a Riner-Rivlin fluid with Joule heating, viscous dissipation and suction/injection, *Central European Journal of Physics*, **11**, 363-374, 2013

[23] S. S. Motsa, Z. G. Makukula, S. Shateyi, Spectral local linearization approach for natural convection boundary layer flow, *Mathematical Problems in Engineering*, **2013**, Article ID 765013, 7 pages, **doi**: 10.1155/2013/765013, 2013

[24] C. M. Ece, Free convection flow about a vertical spinning cone under a magnetic field, *Applied Mathematics and Computation*, **179**, 231-242, 2006

[25] F. G. Awad, P. Sibanda, S. S. Motsa, O. D. Makinde, Convection from an inverted cone in a porous medium with cross-diffusion effects. *Computers and Mathematics with Applications*, **61**, 1431-1441, 2011

[26] P. M. Patil, D. N. Latha, S. Roy,E. Momoniat, Double diffusive convection flow from a vertical exponentially stretching surface in the presence of viscous dissipation, *International Journal of Heat and Mass Transfer*, **112**, 758-766, 2017

[27] T. Watanabe, I. Pop, Effects of viscous dissipation and stress work on the steady two dimensional laminar magnetohydrodynamic forced convection flow

over a non-isothermal wedge, *International Communications in Heat and Mass Transfer*, **20**, 871, 1993

[28] E. Magyari,B. Keller, Heat and mass transfer in the boundary layers on exponentially stretching continuous surface, *Journal of Physics D: Applied Physics*, **32**, 577-585, 1999

[29] B. Bidin, R. Nazar, Numerical solutions of boundary layer flow over an exponentially stretching surface with thermal radiation, *European Journal of Scientific Research*, **33**, 710-717, 2009

[30] S. Mukhopadhyay, Slip effects on MHD boundary layer flows over an exponentially stretching sheet with suction/blowing and thermal radiation, *Ain Shams Engineering Journal*, **4**, 485-491, 2013

[31] I. A. Hassanien, T. H. Al-arabi, Non-Darcy unsteady mixed convection flow near the stagnation point on a heated vertical surface embedded in a porous medium with thermal radiation and variable viscosity. *Commun Nonliner Sci Numer Simulat*, **14**, 1366-1376, 2009

[32] S. S. Motsa, A new spectral relaxation method for similarity variable nonlinear boundary layer flow systems, *Chemical Engineering Communications*, **201**, 241-256, 2014

[33] V. M. Magagula, S. S. Motsa, P. Sibanda, P. G. Dlamini, On the bivariate spectral relaxation method for unsteady magneto-hydrodynamic flow in porous media. *Springer plus*, **doi**: 10.1186/s40064-016-2053-4, 2016

[34] S. S. Motsa, P. G. Dlamini, M. Khumalo, Spectral relaxation method and spectral quasilineariation method for solving unsteady boundary layer flow problems. *Advances in Mathematical Physics*, **doi**:10.1155/2014/341964, 2014

[35] P. Kameswaran, P. Sibanda, S. S. Motsa, A spectral relaxation method for thermal dispersion and radiation effects in a nanofluid flow, *Boundary Value Problems*, **2013**, 2013:242, 2013

[36] T. M. Agbaje, S. S. Motsa, Comparison between spectral perturbation and spectral relaxation approach for unsteady heat and mass transfer by MHD mixed convection flow over an impulsively stretched vertical surface with chemical reaction effect. *Journal of Interpolation and approximation in Scientific Computing*, **2015**, 48-83, 2015

[37] S. Shateyi, On spectral relaxation method for an MHD flow and heat transfer of Maxwell fluid, *International Conference on Mechanics, Heat and Mass Transfer*, **ISBN**: 978-1-61804-220-0, 102-106, 2014

[38] S. S. Motsa, Z. G. Makukula, On spectral relaxation method approach for steady von-Karman flow of a Reiner-Rivlin fluid with Joule heating, viscous dissipation and suction/injection, *Central European Journal of Physics*, **11**: 363-374, 2013